Journal Pre-proofs

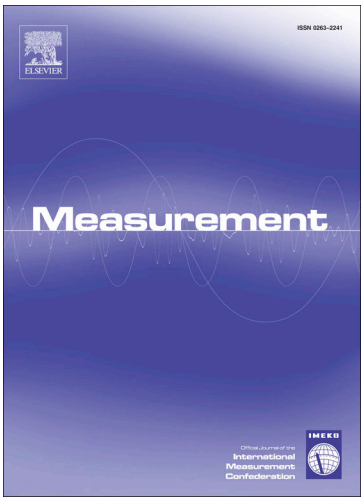

Simultaneous measurement of the moment of inertia and braking torque of electric motors applying additional inertia

Attila SZÁNTÓ, Éva ÁDÁMKÓ, György JUHÁSZ, Gusztáv Áron SZIKI

PII: S0263-2241(22)01331-8
DOI: https://doi.org/10.1016/j.measurement.2022.112135
Reference: MEASUR 112135

To appear in: *Measurement*

Received Date: 14 July 2022
Revised Date: 12 October 2022
Accepted Date: 26 October 2022

Please cite this article as: A. SZÁNTÓ, E. ÁDÁMKÓ, G. JUHÁSZ, G. Áron SZIKI, Simultaneous measurement of the moment of inertia and braking torque of electric motors applying additional inertia, *Measurement* (2022), doi: https://doi.org/10.1016/j.measurement.2022.112135

SIMULTANEOUS MEASUREMENT OF THE MOMENT OF INERTIA AND BRAKING TORQUE OF ELECTRIC MOTORS APPLYING ADDITIONAL INERTIA

Attila SZÁNTÓ, [2]Éva ÁDÁMKÓ, [3]György JUHÁSZ, [4]Gusztáv Áron SZIKI

[1]Faculty of Engineering of the University of Debrecen

szanto.attila@eng.unideb.hu

[2]Faculty of Engineering of the University of Debrecen

adamko.eva@eng.unideb.hu

[3]Faculty of Engineering of the University of Debrecen

juhasz@eng.unideb.hu

[4]Faculty of Engineering of the University of Debrecen

szikig@eng.unideb.hu

Abstract

This paper presents a method for the simultaneous measurement of the moment of inertia and braking torque of the rotor of electric motors. The procedure is based on retardation tests on the motor applying additional loads on its rotor with different moments of inertia but equal masses. The equal masses provide equal braking torques in the supporting bearings. Besides the detailed description of the experimental setup and method – a procedure for determining the optimal values of the loading moments of inertia is also presented. At these optimal values, the errors of the experimentally determined moment of inertia and braking torques are minimal. Additionally, the effect of the temperature change of the bearings on the accuracy and precision of the method is also analyzed and discussed. Finally, the method's experimentally validated accuracy and precision are reported, and measurement results on an induction motor are presented as an example.

Keywords: electric motor, modelling and simulation, moment of inertia, braking torque, retardation test, additional inertia

Introduction

At the Faculty of Engineering of the University of Debrecen, our research group deals with the modelling, simulation and optimization of different types of electric vehicle drives [1, 2, 3]. The gained experience during the last decade is utilized – among others – in university competitions organized for alternative-driven vehicles made by student teams. For more conscious design and racing, a vehicle dynamics simulation program has been developed in MATLAB/Simulink environment [1], which computes the dynamics functions of a vehicle from its technical characteristics and data. Applying the above program – supplemented by an optimizing procedure – the technical parameters and characteristics of a vehicle or its powertrain can be optimized to a given competition task.

A significant part of the simulation program is the simulation of the drive system, including the electric motor [2, 4]. For the simulation of an electric motor, its electromagnetic and dynamic characteristics serve as inputs [2, 4, 5, 6, 7, 8, 9, 10, 11, 12, 13]. The dynamic characteristics include the moment of inertia of the rotor and its braking torque as a function of angular speed. These dynamic characteristics are required as inputs of simulation programs developed in MATLAB/Simulink [4, 5, 9] or in NI LabVIEW Control Designed and Simulation Module [3] and also used as input parameters of other widely used simulation programs such as Ansys-Maxwell RMxprt. The mentioned characteristics

also important for the accurate dynamic modelling and testing of various high-performance motor control strategies [14]. The manufacturers usually do not provide these data; thus, they need to be identified. For the identification there are several options.

1) Measuring the breaking torque as a function of angular speed directly [5, 15, 16], and then determining the moment of inertia of the rotor from a retardation test, using the previously measured function [5]. It must be emphasized, that the direct measurement of braking torque – with an acceptable accuracy – is only possible by applying a torque meter with a very low nominal (rated) torque and value of accuracy class (typically: <0.5 Nm and <0.5%).

2) Measuring the moment of inertia directly, and then determining the braking torque from a retardation test. For measuring the moment of inertia, the most commonly used experimental methods are the pendulum and torsion oscillation methods. It must be emphasized, that these methods can be only applied with acceptable accuracy if the rotor is removed from the motor. Moreover, their application results in significant errors since the rotor has to be well-balanced, and it is difficult to find the centre of gravity or the suspension centre. Removing the rotor is usually time-consuming and can lead to the damage of the motor. Thus, it is not advisable.

3) Identifying the braking torque and moment of inertia simultaneously, without demounting the rotor. For simultaneous identification, different methods exist [14, 17, 18, 19, 20, 21, 22, 23]. In numerous research works, the experimental procedure is supplemented with the application of an appropriate model for the mechanical losses and an algorithm (e.g. genetic algorithm [24]) to find the appropriate values of the parameters [14, 23]. Among the methods – applied for the simultaneous identification – the ones based on retardation tests [14, 18, 19, 20] are relatively easy to use and do not require a complex experimental setup (e.g. a torque meter). Additionally, if the experimental setup and procedure are thoroughly designed and optimized, it is one of the most accurate methods [19]. Thus, our research group decided to apply it, as it was described in [19]. During the application, it was revealed that the procedure is not elaborated in detail enough to be applied with the required accuracy and precision. Consequently, we decided to cope with the problem and improve the method to a well-established, effective analytical procedure. In reference [18], the retardation method is applied, but in the determination of the unknown quantities, the authors neglected mechanical losses which take place in the bearing units of the additional system of rotating masses, as well as the moment of inertia of the bearing units. Thus, the above errors do not allow the determination of the braking torque in an electric motor and determining the moment of inertia of its rotor with high accuracy [19]. In reference [19], the above deficiency was eliminated; thus, the method's accuracy improved. Nevertheless, two significant factors – that have a serious effect on the method's accuracy – haven't been analyzed and considered in reference [19]. Namely, on the one hand, how to determine the optimal values of the moments of inertia of the loading discs, at which the errors of the experimentally determined moment of inertia and braking torques are minimal. On the other hand, the effect of the temperature change of the bearings on the accuracy and precision of the method. Moreover, braking torque values are not presented in reference [19]. Additionally, the expected errors of the experimentally determined moment of inertia haven't been calculated by Gauss' Law of Error Propagation; only a comparison with reference values was performed.

This paper presents a method for simultaneously measuring the moment of inertia and braking torque of electric motors. The method is based on retardation tests on the motor applying additional loads on its rotor in the form of steel discs with different moments of inertia but equal masses. The equal masses provide equal braking torques in the supporting bearings during the measurements. The main advantages of this method are that the rotor does not have to be removed from the motor for the measurements and – if the experimental setup and procedure are thoroughly designed and optimized – its accuracy. An additional advantage is that the braking torque of the bearings can be measured precisely in a wide angular speed range. In Section 1, the detailed description of the experimental setup and method is presented, while in Section 2, the way of data processing and evaluation. In Section 3, the determination of the ideal measurement conditions and procedure are given. On the one hand, the previous includes the determination of the optimal values of the moments of inertia of the loading discs and, on the other hand, the analysis of the effect of the temperature change of the bearings on the accuracy and precision of the method. Finally, in Section 4, the method's experimentally validated accuracy and precision and measurement results on a 3-phase squirrel cage induction motor are presented as an example.

1. Experimental

During the experiments, calibration measurements were performed first to determine the attainable accuracy and precision of the method. After that, measurements on an electric motor were realized. Figure 1a shows the schematic drawing of the experimental setup applied for the calibration measurements, while Figure 1b the one for the determination of an electric motor's unknown moment of inertia.

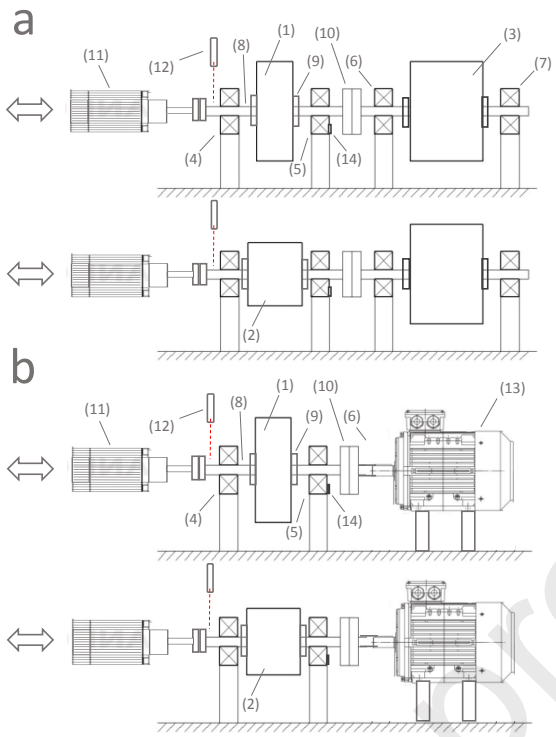

Figure 1. A schematic drawing of the experimental setup was applied for the calibration measurements (a) and the determination of the unknown moment of inertia and braking torque of an electric motor (b).

In Figure 1, steel discs (1) and (2) have equal masses (m) but different moments of inertia (J_1 and J_2). The equal masses provide equal braking torques (M_{brake}) in supporting bearings (4) and (5) at any angular speed value of the rotating system. Steel disc (3) is used for the calibration of the measurement setup and its mass (m_3) and moment of inertia (J_3) are precisely known, while the braking torque (M^*_{brake}) in bearings (6) and (7) are unknown. The discs are fixed to the steel shafts (8) with four clamping rings (9) of the same type, and discs (1) and (2) are connected to disc (3) through a clutch (10). In Table 1, the mass and moment of inertia of each part of the setup are presented. The masses were measured precisely, and the moments of inertia were calculated from the masses and the geometrical data. The masses and the moments of inertia of the two shafts are equal to each other, the mass and the moment of inertia of the inner ring of bearings (4), (5), (6) and (7) are approximated from their geometry and mass density.

	disc (1)	disc (2)	disc (3)	shafts
m [kg]	2.508	2.509	5.030	0.368
J [kg m^2]	0.00222	0.00713	0.00651	0.00004
	clamping rings	inner rings	clutch (10)	
m [kg]	0.136	~ 0.075	0.41	
J [kg m^2]	0.00007	~ 0.00002	0.00018	

Table 1 Masses and moments of inertia of the different rotating parts of the setup

Before each measurement, the proper alignment of the shafts was adjusted by a laser shaft alignment tool. In the course of the calibration measurements, disc (3) – together with its shaft, the two clamping rings and bearings (6) and (7) – play the role of the rotor of the analyzed motor. A drive motor (11) is connected to the system's shaft through a clutch during the measurements. As voltage is switched on the drive motor, the system spins up from rest until it reaches its maximum speed. After that, the connection between the drive motor (11) and the shaft is released, and the system of the rotating masses slows down until it stops. During the retardation of the system, its angular speed is measured by an optical led sensor (12), which receives four light pulses in one full rotation. These pulses are converted to output voltage signals and fed into an NI voltage input module, with an analog input isolation on the channel-to-channel basis, which is connected to a PC through a Compact DAQ Chassis. Applying a self-developed NI LabVIEW program for data collection, the voltage signals were counted, and the angular speed of the system was calculated and displayed as a function of time. The complete experimental procedure includes four measurements. Only disc (1) is connected to the drive motor (11) in the

first one. In the second one, disc (1) and disc (3). (The two discs are connected through a clutch (10).) In the third one, disc (2) together with disc (3), while in the fourth one, only disc (2).

When the unknown moment of inertia and braking torque of an electric motor are measured, the above four experiments must be performed. But disc (3) – together with its shaft, the two clamping rings, and bearings (6) and (7) – are replaced by the analyzed motor (13, Figure 1b). Figure 2a shows a photo of the experimental setup applied for the calibration measurements. Figure 2b is another one of the setups for determining the unknown moment of inertia and braking torque of an electric motor. During each measurement, the surface temperature of the outer ring of bearing (5) was monitored by a PT100 Resistance Temperature Detector (14).

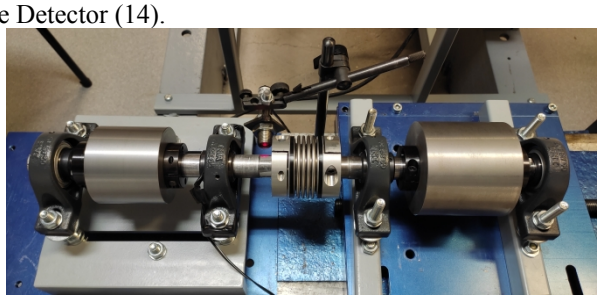

a,

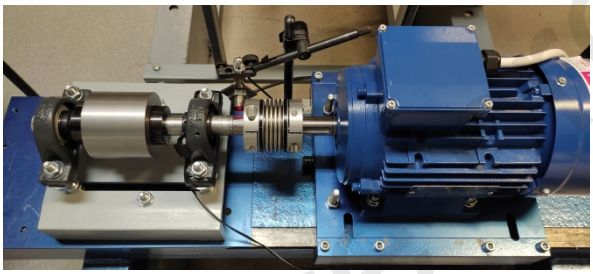

b,

Figure 2 A photo of the experimental setup applied for the calibration measurements (a) and the determination of the unknown moment of inertia and braking torque of an electric motor (b).

2. Data processing and evaluation

The output data of our self-developed NI LabVIEW program is one or more NI LabVIEW measurement (.lvm) files. By default, data are recorded every 0.0001 seconds by the program. Thus, according to the duration of the measurement, a file can contain a few but usually a massive amount of rows of measured data. The measurement files serve as the input of a self-developed Java command-line application that performs filtering by a time gap (usually 0.1-0.2 s) to achieve a much smaller file size. After that, it converts the measurement files into "comma-separated values" (.csv) text files because Microsoft Excel – which was applied for data evaluation – can open that particular type of file. Figure 3 shows the angular speed vs time function of the rotating system when discs (1) and (3) are connected to the drive motor. At the moment 4 s, the connection is released, and the system is gradually slowing down until it stops.

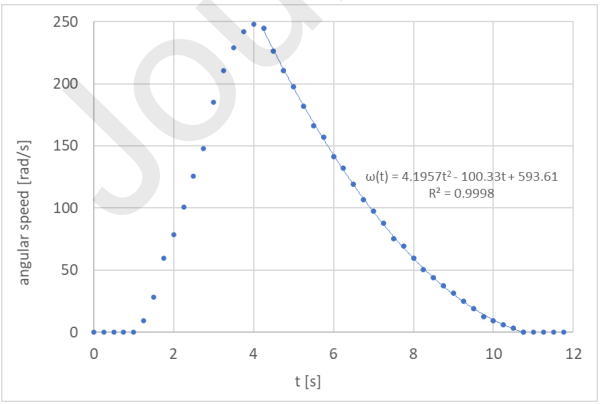

Figure 3 Angular speed vs time function of the system when discs (1) and (3) are connected to the drive motor. The connection is released at the moment 4 s

The measured RPM values were converted to angular speeds, and a quadratic function was fitted to these values during the deacceleration. The rotating systems' angular acceleration vs time functions were calculated by derivation from the fitted functions. After that, the angular acceleration was given as a function of angular speed. Thus, the results of the four experiments are four angular acceleration vs angular speed functions.

Considering the following experimental arrangements during the calibration procedure:

I. disc (1)
II. disc (1) and (3)
III. disc (2)
IV. disc (2) and (3)

are connected to the drive motor, the corresponding dynamic equations during the retardation of the system are:

I. $2 \cdot M_{brake} = (J_1 + J_{add1}) \cdot \varepsilon_1$ /1/
II. $2 \cdot (M_{brake} + M^*_{brake}) = (J_1 + J_3 + J_{add2}) \cdot \varepsilon_{13}$ /2/
III. $2 \cdot M_{brake} = (J_2 + J_{add1}) \cdot \varepsilon_2$ /3/
IV. $2 \cdot (M_{brake} + M^*_{brake}) = (J_2 + J_3 + J_{add2}) \cdot \varepsilon_{23}$ /4/

Where:

$J_{add1} = J_{shaft} + 2 \cdot J_{clpr} + 2 \cdot J_{ring}$ /5/

$J_{add2} = 2 \cdot J_{shaft} + 4 \cdot J_{clpr} + 4 \cdot J_{ring} + J_{clutch}$ /6/

In the equations above M_{brake} and M^*_{brake} are the braking torques in bearings (4) or (5) and (6) or (7), J_1, J_2, J_3, J_{shaft}, J_{clpr}, J_{clutch}, J_{ring} are the moments of inertia of disc (1), disc (2), disc (3), one shaft, one clamping ring, the clutch and one inner ring of a bearing, respectively, ε_1, ε_{13}, ε_2, ε_{23} are the angular accelerations of the four rotating systems during the retardation tests.

From the system of equations above, the moment of inertia of disc (3) and the braking torque in bearing (6) or (7) are:

$$J_3 = \frac{J_2 \cdot \varepsilon_{23} - J_1 \cdot \varepsilon_{13}}{(\varepsilon_{13} - \varepsilon_{23})} - J_{add2} \quad /7/$$

$$M^*_{brake} = (J_2 - J_1) \cdot \frac{\varepsilon_{13} \cdot \varepsilon_{23}}{2 \cdot (\varepsilon_{13} - \varepsilon_{23})} - (J_1 + J_{add1}) \cdot \frac{\varepsilon_1}{2} \quad /8/$$

Applying Gauss' Law of Error Propagation, the error of J_3 and M^*_{brake} can be given as:

$$\Delta J_3 = \sqrt{\left(\frac{\varepsilon_{23} \cdot (J_1 - J_2)}{(\varepsilon_{13} - \varepsilon_{23})^2}\right)^2 \cdot \sigma^2_{\varepsilon_{13}} + \left(\frac{\varepsilon_{13} \cdot (J_2 - J_1)}{(\varepsilon_{13} - \varepsilon_{23})^2}\right)^2 \cdot \sigma^2_{\varepsilon_{23}}} \quad /9/$$

$$\Delta M^*_{brake} = \frac{\sqrt{(J_2 - J_1)^2 \cdot \left(\varepsilon_{23}{}^4 \cdot \sigma^2_{\varepsilon_{13}} + \varepsilon_{13}{}^4 \cdot \sigma^2_{\varepsilon_{23}}\right) + (J_1 + J_{add1})^2 \cdot \sigma^2_{\varepsilon_1}}}{2 \cdot (\varepsilon_{13} - \varepsilon_{23})^2} \quad /10/$$

In Equation /9/ and /10/ $\sigma_{\varepsilon_{13}}$, $\sigma_{\varepsilon_{23}}$ and σ_{ε_1} are the standard deviations of ε_{13}, ε_{23} and ε_1. These deviations were determined from angular accelerations at a given angular speed value obtained from five repeated measurements under the same experimental conditions.

3. Determination of the ideal measurement conditions and procedure

Considering Equation /9/, it can be stated that the error of the experimentally determined moment of inertia of disc (3) depends on the standard derivations of the measured angular accelerations and the moments of inertia of discs (1) and (2). Thus, to be able to minimize the above error, we need to minimize the standard deviations of the measured angular accelerations and find the optimal values of J_1 and J_2 at which the above error is minimal.

Expressing ε_{13} and ε_{23} from Equations /2/ and /4/ and substitute them into Equation /9/ we get:

$$\Delta J_3 = \frac{(J_1 + J^*) \cdot (J_2 + J^*)}{(J_2 - J_1) \cdot M^*} \cdot \sqrt{(J_1 + J^*)^2 \cdot \sigma^2_{\varepsilon_{13}} + (J_2 + J^*)^2 \cdot \sigma^2_{\varepsilon_{23}}} \quad /11/$$

where:

$$J^* = J_3 + J_{add2} \quad /12/$$

$$M^* = 2 \cdot (M_{brake} + M^*_{brake}) \quad /13/$$

The ratio of $\sigma_{\varepsilon_{23}}$ and $\sigma_{\varepsilon_{13}}$ is approximately constant on the $[50;150]$ rad s^{-1} angular speed range; thus, we can introduce constant r as:

$$r = \frac{\sigma_{\varepsilon_{23}}}{\sigma_{\varepsilon_{13}}} \quad /14/$$

Thus:

$$\Delta J_3 = \frac{(J_1 + J^*) \cdot (J_2 + J^*) \cdot \sigma_{\varepsilon_{13}}}{(J_2 - J_1) \cdot M^*} \cdot \sqrt{(J_1 + J^*)^2 + (J_2 + J^*)^2 \cdot r^2} \quad /15/$$

Substituting the average values of J^*, M^*, $\sigma_{\varepsilon_{13}}$ and $\sigma_{\varepsilon_{23}}$ (see Table 2) into Equation /15/:

$$\Delta J_3 = \frac{(J_1 + 0.0071) \cdot (J_2 + 0.0071) \cdot \sqrt{(J_1 + 0.0071)^2 + (J_2 + 0.0071)^2 \cdot 1.626^2}}{(J_2 - J_1) \cdot 0.9666} \quad /16/$$

The average values were calculated from the values on the $[75,100]$ rad s^{-1} angular speed range.

Table 2:

$J^*[kg\ m^2]$	$M^*[Nm]$	$\sigma_{\varepsilon_{13}}[rad\ s^{-2}]$	$\sigma_{\varepsilon_{23}}[rad\ s^{-2}]$
0.00710	0.580	0.60	0.3690

Figure 5 shows the relative percentage error of the experimentally determined value of J_3 as a function of J_1 and J_2:

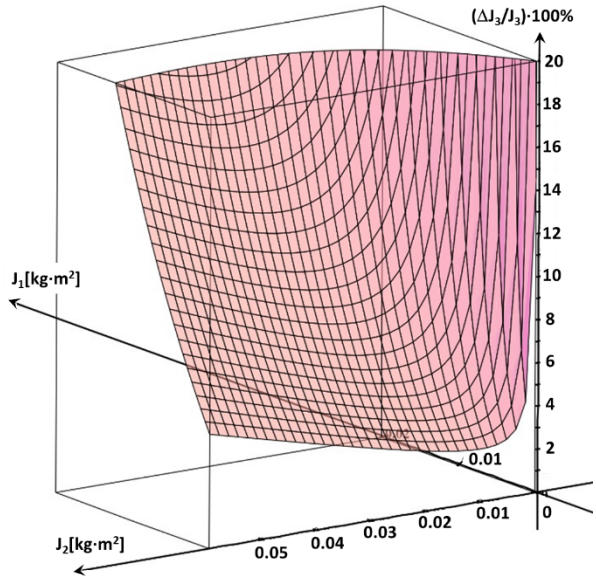

Figure 5 The relative percentage error of the experimentally determined value of J_3 as a function of J_1 and J_2

In Figure 6, the relative percentage error of J_3 is given as the function of J_1 at different fixed J_2 values.

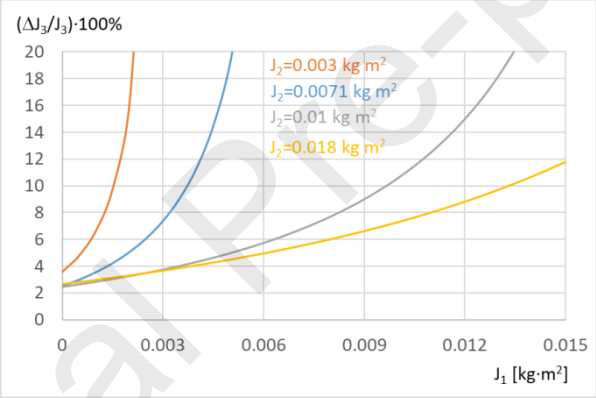

Figure 6 Relative percentage error of J_3 given as the function of J_1 at different fixed J_2 values

It can be seen that with the optimal selection of the moments of inertia of discs (1) and (2), the relative percentage error of the experimentally determined value of J_3 can be reduced below 4%. Further reduction can be achieved by reducing the standard deviations of the experimentally determined angular acceleration values. It must be emphasized that the above standard deviations strongly depend on the temperature change of the bearings during a series of measurements. The reason for that is the strong dependence of the oil's viscosity in the bearing, therefore braking torque, on temperature. Systematic measurements were performed to demonstrate the above dependence: Voltage was switched on the drive motor, and disc (2) was spinning up from rest until it reached its maximum speed. After that, the connection between the drive motor and the shaft was released, and the system slowed down until it stopped. It was repeated five times. Immediately after, the system was forced to rotate at its maximum speed for one minute. Then, the whole procedure was repeated five times. During the experiment, the surface temperature of the outer ring of bearing (5) and the angular speed of the rotating system were measured. Figure 7 shows the obtained results:

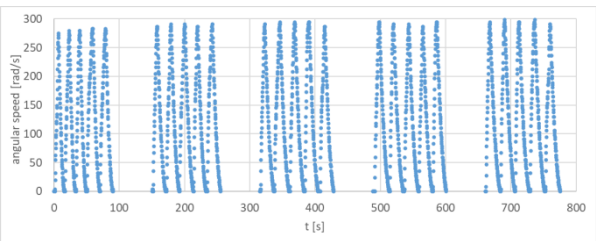

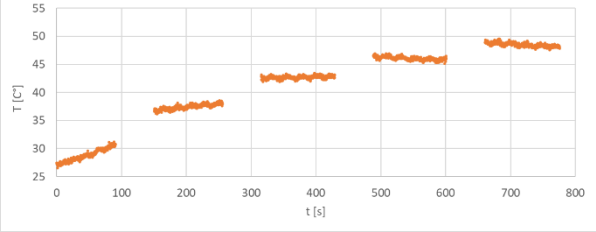

Figure 7 The angular speed values of disc (2) and the surface temperature of the outer ring of bearing (5) as a function of time

To demonstrate the dependence of braking torque in bearing (5) on temperature, its value was calculated from the measured angular speed vs time functions – during the 25 deceleration phases – at three different angular speed values applying formula /3/. Figure 8 shows the obtained results.

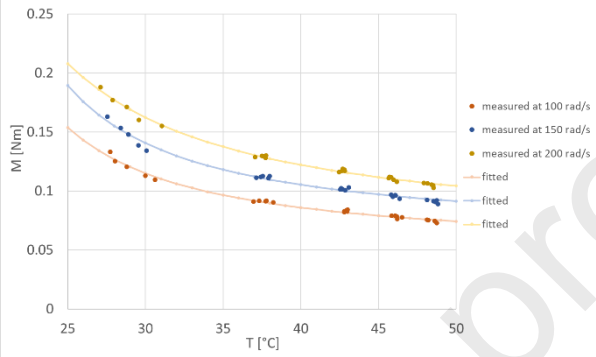

Figure 8 Braking torque in bearing (5) as a function of temperature at three different angular speed values. The temperature was measured on the surface of the outer ring of the bearing.

Figure 8 demonstrates the strong dependence of braking torque on the temperature at different fixed angular speed values. The only reason for that dependence is the dependence of the oil's viscosity in the bearing on temperature. The temperature dependence of the above viscosity is given by the Vogel–Fulcher–Tammann (VFT) formula [25, 26]. Since braking torque is proportional to that viscosity, we applied a similar formula to VFT (Equation /17/) for fitting the measured data in Figure 8.

$$M(T) = A \cdot e^{\frac{B}{T-C}} \qquad /17/$$

In the above formula A, B and C are parameters for the regression and T is the temperature measured on the outer ring of the bearing. Changing temperature, thus, changing braking torque during a series of measurements dramatically increases the standard deviation of the measured angular accelerations, hence the error of the experimentally determined moment of inertia and braking torque. To avoid this situation, the temperature changes of the bearings have to be minimized. It can be realized by applying long breaks between two subsequent measurements, thus letting the bearings cool down. If very high angular speed values are required, it is advised to reduce the time required to spin up the bearing, as much as it is possible, and it can be necessary to cool supporting bearings (4), (5), (6) and (7). In the case of our measurements, the maximum speed was 120 rad s^{-1}, and 5 minutes breaks were applied between two subsequent measurements.

4. Results

Figure 9 shows the experimentally determined moment of inertia of disc (3) (brown markers) at different angular speed values. It's certified value is also marked in the figure as a blue line.

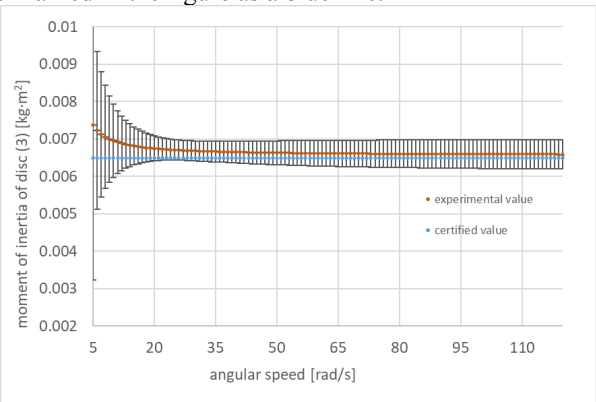

Figure 9 The experimentally determined and certified values of the moment of inertia of disc (3)

The experimental values were calculated from the measured angular accelerations (ε_{13}, ε_{23}) substituting them into Equation /7/. The marked errors in the figure were calculated applying formula /9/ from the measured values of ε_{13} and ε_{23} and their standard deviations ($\sigma_{\varepsilon_{13}}$, $\sigma_{\varepsilon_{23}}$). It can be seen that the obtained values are independent of the angular speed of the rotating system in the $[50;120]\ \mathrm{rad\,s^{-1}}$ range. The experimentally determined value in the above range is: $J_3 = 0.00661 \pm 0.00035\ \mathrm{kg\,m^2}$, which is in a good agreement with the certified one: $0.00650\ \mathrm{kg\,m^2}$. Thus, the relative percentage error of the experimental value is 5.3%. In Figure 10, the sum of the braking torques in bearings (6) and (7) is presented as the function of angular speed. During the measurement, the temperature of the bearings was about 26 C° and the sum of the normal loads on them was approximately 50 N.

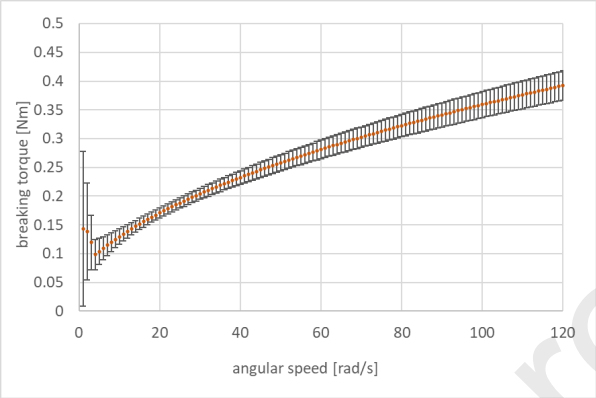

Figure 10 The sum of the braking torques in bearings (6) and (7) as a function of angular speed $(\mathrm{T} = 26\ \mathrm{C}^{\circ})$

The values and errors in Figure 10 were calculated by Equation /8/ and /10/, respectively. The relative percentage error of the experimentally determined braking torques is varied between 5-6% in the $[20;120]\ \mathrm{rad\,s^{-1}}$ angular speed range. In Figures 10 and 12, the presented braking torques are the sum of the friction torques of the bearings and the windage torques. In case of Figure 10 the windage torques are presumably negligible. The friction behaviour in lubricated bearings is characterized by the Stribeck curve [27]. If the normal load on the bearing and the lubricant's viscosity have a fixed value, this curve gives the coefficient of friction (or the friction torque which is linearly proportional to it) of the bearing as the function of angular speed. The Stribeck curve is traditionally divided into three angular speed ranges: boundary lubrication, mixed lubrication, and hydrodynamic lubrication regimes. In Figures 10, the hydrodynamic lubrication regime can be clearly identified. The mixed lubrication regime can be also identified with the high increase of bearing friction torque at low angular speed, but in this regime the values are characterized with a large error.
Figures 11 and 12 show the experimentally determined moment of inertia and braking torque of the analyzed 3 phase squirrel cage induction motor at different angular speed values.

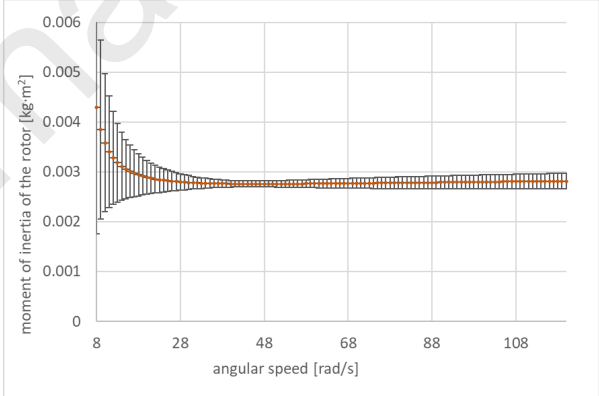

Figure 11 The experimentally determined values of the moment of inertia of the rotor of the analyzed 3 phase squirrel cage induction motor

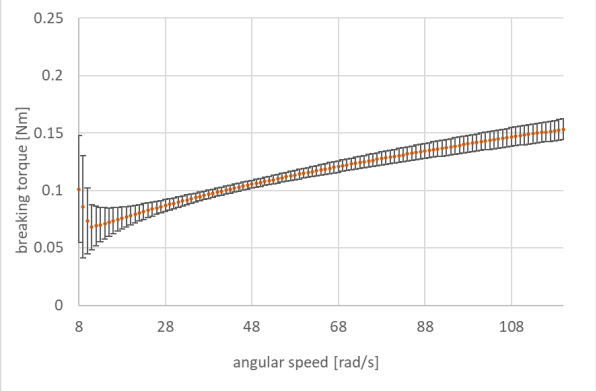

Figure 12 The braking torque of the rotor of the analyzed 3 phase squirrel cage induction motor as a function of angular speed (T = 26 C°)

The presented values in Figure 11 were calculated by Equation /7/, while their errors by Equation /9/, but in the case of these measurements J_{add2} is calculated as:

$$J_{add2} = J_{shaft} + 2 \cdot J_{clpr} + 2 \cdot J_{ring} + J_{clutch} \quad /17/$$

The experimentally determined average value of the moment of inertia of the rotor in the $[50;120] \mathrm{rad\ s^{-1}}$ range is: $J_{rotor} = 0.0028 \pm 0.00012\ \mathrm{kg\ m^2}$. Thus, the relative percentage error is 4.3%. The presented braking torque values in Figure 12 were calculated by Equation /8/, while their errors by Equation /10/, but in both cases, they were multiplied by 2. The relative percentage error of the experimentally determined braking torques is varied between 3-6% in the $[30;120]\ \mathrm{rad\ s^{-1}}$ angular speed range.

5. Conclusion

A novel method for the simultaneous measurement of the moment of inertia and braking torque of the rotor of electric motors was presented. The method is based on retardation tests on the motor applying additional loads – in the form of steel discs – on its rotor with different moments of inertia but equal masses. The optimal values of these loading moments of inertia – at which the experimental errors of the measured quantities are minimal – were determined by a graphic procedure applying Gauss's law of error propagation. Moreover, it was proved that the temperature changes in the bearings – during a series of measurements – dramatically increase the experimental errors of the measured quantities. Nevertheless, if the measurements are carried out at a constant temperature of the bearings and the optimal values of the loading moments of inertia are applied, the experimental errors can be minimized. Under optimal measurement conditions, the certified relative accuracy of the method for the measurement of moment of inertia is 4.3-5.3%, while for the measurement of braking torque is 3-6% in the $[30;120]\ \mathrm{rad\ s^{-1}}$ angular speed range. Under $30\ \mathrm{rad\ s^{-1}}$ angular speed, the experimental errors are significantly higher.

The advantages of the presented method are that it is relatively easy to use and does not require a complex experimental setup (e.g. a torque meter), nor the modelling of the mechanical losses and the application of algorithms to find the appropriate values of the dynamic parameters. Additionally, if the experimental setup and procedure are thoroughly designed and optimized, it is one of the most accurate methods.

Acknowledgement

"SUPPORTED BY THE ÚNKP-21-3 NEW NATIONAL EXCELLENCE PROGRAM OF THE MINISTRY FOR INNOVATION AND TECHNOLOGY FROM THE SOURCE OF THE NATIONAL RESEARCH, DEVELOPMENT AND INNOVATION FUND."

"SUPPORTED BY THE ÚNKP-21-4-II NEW NATIONAL EXCELLENCE PROGRAM OF THE MINISTRY FOR INNOVATION AND TECHNOLOGY FROM THE SOURCE OF THE NATIONAL RESEARCH, DEVELOPMENT AND INNOVATION FUND."

"THE RESEARCH WAS SUPPORTED BY THE THEMATIC EXCELLENCE PROGRAMME (TKP2020-NKA-04) OF THE MINISTRY FOR INNOVATION AND TECHNOLOGY IN HUNGARY."

References

[1] Szántó, Attila, Sándor Hajdu, and Gusztáv Aron Sziki. "Dynamic simulation of a prototype race car driven by series wound DC motor in Matlab-Simulink." Acta Polytech. Hung 17.4 (2020): 103-22.

[2] Síki, Gusztáv Áron, Attila Szántó, and Tamás Mankovits. "Dynamic modelling and simulation of a prototype race car in MATLAB/Simulink applying different types of electric motors." International Review of Applied Sciences and Engineering 12.1 (2021): 57-63.

[3] Síki, Gusztáv Áron, et al. "Series Wound DC Motor Simulation Applying MATLAB SIMULINK and LabVIEW Control Design and Simulation Module." Periodica Polytechnica Transportation Engineering 48.1 (2020): 65-69.

[4] Sziki, Gusztáv Áron, et al. "Experimental investigation of a series wound dc motor for modeling purpose in electric vehicles and mechatronics systems." Measurement 109 (2017): 111-118.

[5] Hadžiselimović, Miralem, et al. "Magnetically nonlinear dynamic model of a series wound DC motor." PRZEGLĄD ELEKTROTECHNICZNY (Electrical Review), ISSN (2011): 0033-2097.

[6] Miss Avanti, B. Tayade. "Modeling and Simulation of A Bldc Motor By Using Matlab/Simulation Tool." Journal of Electrical and Electronics Engineering, e-ISSN (2014): 2278-1676.

[7] Gencer, C., and M. Gedikpinar. "Modeling and simulation of BLDCM using MATLAB/SIMULINK." Journal of Applied Sciences 6.3 (2006): 688-691.

[8] Jambulingam, Vikramarajan. "Mathematical Modelling and Simulation of Brushless DC Motor Using MATLAB." International Journal for Research in Applied Science & Engineering Technology (IJRASET) 3 (2015).

[9] El Shewy, H. M., et al. "Dynamic modeling of permanent magnet synchronous motor using MATLAB-simulink." The International Conference on Electrical Engineering. Vol. 6. No. 6th International Conference on Electrical Engineering ICEENG 2008. Military Technical College, 2008.

[10] Rechkemmer, Sabrina K., Weimin Zhang, and Oliver Sawodny. "Modeling of a permanent magnet synchronous motor of an e-scooter for simulation with battery aging model." IFAC-PapersOnLine 50.1 (2017): 4769-4774.

[11] Mohan, Ned. Advanced electric drives: analysis, control, and modeling using MATLAB/Simulink. John wiley & sons, 2014.

[12] Shi, K. L., et al. "Modelling and simulation of the three-phase induction motor using simulink." International journal of electrical engineering education 36.2 (1999): 163-172.

[13] Aktaibi, Adel, and M. A. Rahman. "Dynamic simulation of a three-phase induction motor using matlab simulink." currents 8 (2011): 9.

[14] Reljić, D. D., & Jerkan, D. G. (2014). Experimental identification of the mechanical parameters of an induction motor drive. In Proceedings of the X international symposium on industrial electronics (INDEL 2014) (pp. 106-114).

[15] Pfister, Pierre-Daniel, and Yves Perriard. "Very-high-speed slotless permanent-magnet motors: Analytical modeling, optimization, design, and torque measurement methods." IEEE Transactions on industrial electronics 57.1 (2009): 296-303.

[16] Li, Silong, et al. "High-speed electric machines: Challenges and design considerations." IEEE Transactions on Transportation Electrification 2.1 (2016): 2-13.

[17] Despalatović, Marin, Martin Jadrić, and Božo Terzić. "Identification of induction motor parameters from free acceleration and deceleration tests." Automatika: časopis za automatiku, mjerenje, elektroniku, računarstvo i komunikacije 46.3-4 (2005): 123-128.

[18] Podzharenko, Vladimir A., and Vladimir Yu Kucheruk. "New method of measurement of a moment of inertia of an electrical machines." XIV IMEKO World Congress.–Tampere (Finland). Vol. 3. 1997.

[19] Egorov, Aleksey V., Konstantin E. Kozlov, and B. N. Belogusev. "Experimental identification of the electric motor moment of inertia and its efficiency using the additional inertia." ARPN Journal of Engineering and Applied Sciences 11.17 (2016): 10582-10588.

[20] Ilina, Ion Daniel. "Experimental determination of moment to inertia and mechanical losses vs. speed, in electrical machines." 2011 7th International Symposium on Advanced Topics in Electrical Engineering (ATEE). IEEE, 2011.

[21] Lekurwale, Rahul A., and S. G. Tarnekar. "Determination of Moment of Inertia of Electrical Machines using MATLAB." International Journal of Engineering Research & Technology (IJERT) 1.10 (2012): 2278-0181.

[22] Yang, S. M., & Deng, Y. J. (2005, October). Observer-based inertial identification for auto-tuning servo motor drives. In Fourtieth IAS Annual Meeting. Conference Record of the 2005 Industry Applications Conference, 2005. (Vol. 2, pp. 968-972). IEEE.

[23] Alonge, F., D'Ippolito, F., Ferrante, G., & Raimondi, F. M. (1998). Parameter identification of induction motor model using genetic algorithms. IEE Proceedings-Control Theory and Applications, 145(6), 587-593.

[24] Holland, J. H. (1992). Adaptation in natural and artificial systems: an introductory analysis with applications to biology, control, and artificial intelligence. MIT press.

[25] D. H. Vogel, "Das Temperaturabhaengigkeitsgesetz der Viskositaet von Fluessigkeiten," Physikalische Zeitschrift, Vol. 22, 1921, p. 645.

[26] Garca-Coln, L. S., L. F. Del Castillo, and Patricia Goldstein. "Theoretical basis for the Vogel-Fulcher-Tammann equation." Physical Review B 40.10 (1989): 7040.

[27] Lu, Xiaobin, M. M. Khonsari, and E. R. M. Gelinck. "The Stribeck curve: experimental results and theoretical prediction." (2006): 789-794.

Attila SZÁNTÓ: investigation, formal analysis, methodology, visualization, writing - original draft

György JUHÁSZ: resources, conceptualization, data curation, visualization

Éva ÁDÁMKÓ: software, formal analysis, data curation, writing – review and editing

Gusztáv Áron SZIKI: conceptualization, investigation, formal analysis, methodology, visualization, validation, writing – original draft, supervision

Declaration of interests

☒ The authors declare that they have no known competing financial interests or personal relationships that could have appeared to influence the work reported in this paper.

☐ The authors declare the following financial interests/personal relationships which may be considered as potential competing interests:

Highlights

- Simultaneous measurement of moment of inertia and braking torque of electric motors
- Realization by optimized retardation tests applying additional inertia as loading
- Determining optimal loading moments of inertia by a graphical method
- Temperature changes in bearings dramatically increase experimental errors
- At optimal conditions the relative accuracy of measured quantities is 3-5%